

E1 transition probabilities from $K^\pi = 0^-$ and $K^\pi = 1^-$ states of ^{238}Pu

C. Michael Lederer

Lawrence Berkeley Laboratory, University of California, Berkeley, California 94720

(Received 13 March 1981)

Levels of ^{238}Pu were studied in the β^- decay of ^{238}Np and the α decay of ^{242}Cm . Thirteen γ -ray transitions were observed for the first time, and additional information about multiplicities and mixing ratios was obtained. An analysis of the γ -ray branching ratios gives a measure of the E1 transition probabilities between octupole-vibrational states and the ground-state band, corresponding to $F_W = 4.3 \times 10^4$ for $\Delta K = 1$ transitions and $F_W = 1.5 \times 10^4$ for $\Delta K = 0$. The latter transitions are three orders of magnitude faster than those that occur in the isotone ^{236}U , for which $F_W(\Delta K = 0) = 2.2 \times 10^7$, from a direct measurement of the half-life of the $0, 1^-$ state. Estimates of the hindrance factors for E1 transitions from octupole states in other heavy nuclei are given, and the validity of the calculations on which they are based is discussed.

[RADIOACTIVITY ^{238}Np [from $^{237}\text{Np}(n, \gamma)$] measured $E_\gamma, I_\gamma, I_{cp}, ICC, ^{242}\text{Cm}$ [from $^{214}\text{Am}(n, \gamma)^{242}\text{Am}(\beta^-)$] measured $E_\gamma, I_\gamma, ^{238}\text{Pu}$ deduced levels, $J^\pi, t_{1/2}$ (levels). Ge(Li) and Si(Li) detectors.]

I. INTRODUCTION

Studies of the reactions $^{235}\text{U}(d, p\gamma), ^{236}\text{U}(d, d'), ^2$ and Coulomb excitation³ support an assignment of $K, I^\pi = 0, 1^-$ for the 688-keV state of ^{236}U , rather than $2, 2^-$, as proposed from decay-scheme studies.^{4,5} The high conversion coefficients for E1 transitions deexciting the state, which were the main evidence supporting the $2, 2^-$ assignment, can be understood generally in terms of the systematics of anomalous conversion⁶⁻⁸ (see Fig. 1), although the observed anomaly in the L_{III} conversion coefficients⁴ is inconsistent with the normal $\alpha(L_{III})$ values for other anomalously converted transitions,⁶ and is in serious conflict with theory. [An anomalous value of $\alpha(L_{III})$ for the 642-keV transition in ^{236}U is statistically well established⁴; however, it is possible that an impurity line is responsible. Further study of this point is required.] Given the $0, 1^-$ assignment, the high hindrance of the E1 transitions is inconsistent with the macroscopic description of the state as an octupole-vibrational shape excitation. The theoretical description of such a state includes significant mixing with the giant dipole excitation, resulting in E1 strengths of 10^{-2} to 10^{-3} Weisskopf units,⁹⁻¹¹ compared to 10^{-7} in ^{236}U .

There is qualitative evidence that the E1 transitions in ^{236}U are "anomalous" compared to those in neighboring nuclides: (1) only in ^{236}U does the intraband E2 transition dominate the deexcitation of the $0, 3^-$ state so completely that no E1 transitions are observed from that state; (2) no other case of anomalous conversion of E1 transitions from octupole states of heavy nuclei is known. [Conversion coefficients or limits have been mea-

sured for $\Delta K = 0$ E1 transitions in most of the nuclides listed in Table V and several others (see Ref. 8). The measured limit is less than twice the theoretical value in all cases, and, in the best-measured cases, α_K is equal to the theoretical value to within 10 percent. By contrast, the K and L_{I+II} conversion coefficients of the 688-keV transition in ^{236}U and 37 and 67 times the theoretical values, respectively.] Better estimates of E1 transition rates in this region are

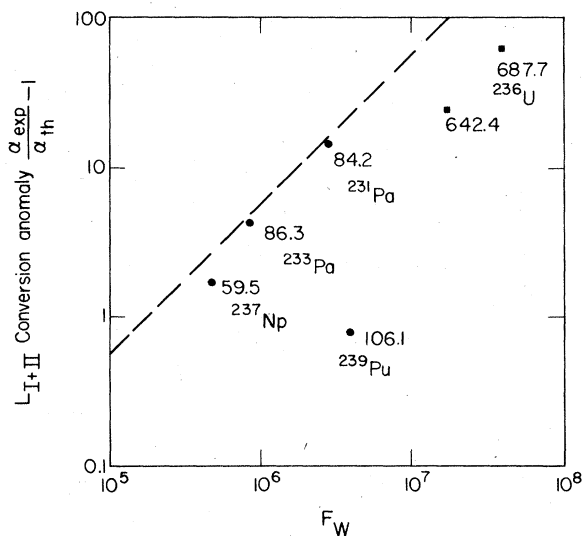


FIG. 1. Internal conversion anomaly versus Weisskopf hindrance factor for some anomalous E1 transitions in the actinide region. The Weisskopf factors are calculated as described in the text. The dashed line is an approximate upper limit from systematics and the theoretical model for anomalous conversion (Ref. 6).

generally lacking, due to an absence of direct half-life measurements. Peker and Hamilton¹² reviewed some transition-rate and branching-ratio data in spherical as well as deformed nuclei, and concluded that the $E1$ transitions are not collective. The systematics of the isotopes of radium through plutonium are of special interest, because the octupole states in this region have very low, smoothly varying energies characteristic of collective states.

The present study of the decay of ^{238}Np and ^{242}Cm provides new data sufficient to permit estimates of the $E1$ lifetimes for the $K=0$ and $K=1$ octupole states in ^{238}Pu , by comparison of the $E1$ intensities with the intensities of competing, rotation-admixed transitions ($K^\pi = 1^- \rightarrow K^\pi = 0^-$) whose rates can be calculated from theory. In Sec. IV, this calculation is developed and applied to other nuclei for which sufficient data exist.

II. SOURCES AND INSTRUMENTATION

Sources of ^{238}Np were prepared by irradiation of $^{237}\text{NpO}_2(\text{NO}_3)$ in the University of California Triga reactor at a flux of 10^{13} neutrons per cm^2s for about 1 day. The resulting activity was purified by anion exchange of the chloride complex, and thin sources for electron spectroscopy were prepared by vacuum sublimation onto a 0.025-mm thick aluminum backing. Collimators used to define the area of the electron source served as gamma-ray sources for most measurements.

The gamma-ray spectrum was measured using three different detector systems: a 12 cm^3 Ge(Li) detector with a resolution of 2.3 keV at 1 MeV, a 1 cm^3 Ge(Li) detector with a resolution of 1.6 keV at 1 MeV, and a Ge(Li) Compton suppression spectrometer at Lawrence Livermore Laboratory with a resolution of 2.2 keV at 1 MeV. Conversion electrons were studied with a 5-mm thick by 1 cm^2 Si(Li) detector with a resolution of 2.6 keV at 1 MeV. Electrons coincident with K x rays were measured with the Si(Li) detector and a 3.8×3.8 -cm NaI(Tl) scintillator.

A source of ^{242}Cm was prepared by irradiation of 30 mg of pure ^{241}Am at a flux of 10^{14} neutrons per cm^2s for 2 weeks. The resulting sources contained ^{242}Cm and ^{243}Cm (from neutron capture by ^{242}Cm) in an activity ratio 1.8×10^{-6} . Americium and curium were separated from fission products by elution from a cation-exchange column with HCl-saturated ethanol; curium was then separated from the americium by elution from a cation-exchange column with 0.28 M α -hydroxyisobutyric acid buffered to a pH of 4.8 at 87°C . Sources were evaporated to dryness as CmCl_3 in a Pyrex tube, and sealed under helium at 1 atm.

The helium atmosphere suppresses nuclear reactions induced by ^{242}Cm α particles, particularly the reaction $^{14}\text{N}(\alpha, p)^{17}\text{O}^*$, which yields an 871-keV γ ray that is intense compared to the weak ^{242}Cm γ rays. The γ -ray spectrum of ^{242}Cm was studied with the 12 cm^3 Ge(Li) detector.

Gamma-ray energies were calibrated with standards measured before and after or, in some experiments, simultaneously with the ^{238}Np or ^{242}Cm source. The photopeak efficiency functions of the detectors had been calibrated previously with sources whose absolute or relative γ -ray emission rates were known to $\pm 1\%$. The electron-energy scale was calibrated with the measured γ -ray energies of stronger lines. The efficiency of the electron detector has been shown to be linear in the region of interest (≤ 1 MeV) by measurement of electrons from ^{207}Bi and $^{180}\text{Hf}^m$ decay.¹³

III. EXPERIMENTAL RESULTS

A. ^{238}Np decay

The γ -ray spectrum was studied primarily with the 12 cm^3 and Compton suppression spectrometers. Several closely-spaced lines were studied also with the 1 cm^3 detector; Fig. 2 shows the spectrum in the region of the 936.61- and 941.38-keV γ rays, analysis of which indicates the likely presence of the weak 938.95-keV γ ray. Table I lists the measured energies and intensities and

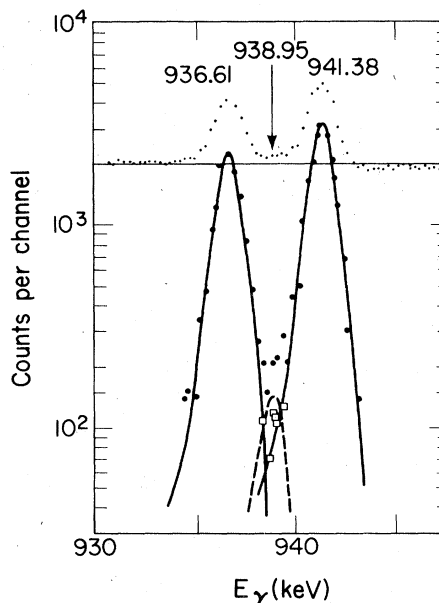


FIG. 2. A small portion of the γ -ray spectrum of ^{238}Np taken with the 1 cm^3 Ge(Li) detector. The weak 938.95-keV line, inferred to be present from the computer analysis shown in the figure, was seen clearly in the decay of ^{242}Cm .

TABLE I. Gamma rays of ^{238}Np .

Present work	E_γ (keV)		Present work ^d	I_γ (%) ^c		I_{trans} (%) ^e
	Winter <i>et al.</i> ^a	Adopted ^b		Winter <i>et al.</i> ^a		
	44.08(3)	44.08(3)	0.09(1) ^f	≈ 0.05	79(4)	
	$K\alpha_2$ x ray		0.20(1)	0.18		
101.93(4)	101.88(2)	101.90(3) ^g	0.27(1)	0.245(6)	4.3(2)	
	$K\alpha_1$ x ray		0.30(1)	0.29		
	114.4(4)	114.4(4)		0.006(1)	0.057(9)	
119.9(1)	120.14	119.9(1) ^h	0.103(7)	0.114(6)	0.48(3)	
132.49(11)	132.6(6)	132.49(11) ^h	0.0028(2)	0.0032(19)	0.0035(3)	
157.4(3)?		157.42(5) ⁱ	≈ 0.001		≈ 0.003	
173.78(11)	174.06(8)	174.0(2) ^j	0.026(1)	0.031(3)	0.030(1)	
220.87(11)		220.87(11) ^{h, n}	0.0034(4)		0.042(5)	
301.19(12)	301.81(19)	301.4(3) ^j	0.012(1)	0.014(3)	0.015(1)	
319.29(11)		319.29(11) ^h	0.009(1)		0.015(3)	
321.75(20)		321.75(20) ^h	0.0013(6)		0.0013(6)	
323.95(9)	324.08(17)	323.98(9) ^j	0.016(1)	0.019(3)	0.020(2)	
357.60(9)	357.64(7)	357.62(7) ^j	0.053(3)	0.061(6)	0.064(4)	
378.05(13)		378.05(13) ^h	0.0033(6)		0.0034(6)	
380.28(13)	380.33(22)	380.29(13) ^j	0.0120(6)	0.014(3)	0.013 to 0.020	
421.15(11)	421.12(16)	421.14(11) ^j	0.023(1)	0.027(3)	0.025 to 0.035	
459.8(2)?		459.80(22) ⁱ	≈ 0.003		≈ 0.003	
515.58(12)	515.47(17)	515.5(2) ^g	0.043(2)	0.039(6)	0.043(2)	
561.09(10)	561.15(7)	561.11(7) ^g	0.114(2)	0.120(6)	0.115(5)	
605.24(13)	605.14(9)	605.13(9) ^g	0.079(4)	0.086(8)	0.079(4)	
617.45(12)	617.39(11)	617.36(11) ^{g, k}	0.074(4)	0.081(8)	0.075(4)	
837.18(15)	837.0(4)	837.11(15) ⁱ	0.028(2)	0.021(6)	0.028(2)	
882.65(7)	882.63(3)	882.63(3)	0.87(3)	0.89(4)	0.88(3)	
897.28(20)		897.33(10) ⁱ	0.008(1)	<0.01	0.008(1)	
918.70(7)	918.69(4)	918.69(4)	0.59(2)	0.060(3)	0.59(2)	
923.99(6)	923.98(2)	923.98(2)	2.86(9)	2.89(14)	2.90(9)	
936.57(9)	936.61(6)	936.61(6)	0.40(1)	0.39(2)	0.40(1)	
939.00(10)	938.6(5)	938.95(10) ⁱ	0.026(3) ^m	0.036(17)	0.141(6)	
941.39(6)	941.38(5)	941.38(5)	0.55(2)	0.53(3)	0.55(2)	
941.5(3)		941.5(3) ^h	(pure E0)		0.012(2)	
962.80(7)	962.77(3)	962.77(3)	0.70(2)	0.71(4)	0.70(2)	
	968.9(4)	968.9(4)	<0.04	0.017(6)	0.019(6)	
984.46(7)	984.45(2)	984.45(2)	27.8	(27.8)	28.2	
1025.87(6)	1025.87(2)	1025.87(2)	9.7(6)	9.6(5)	9.9(6)	
1028.54(6)	1028.54(2)	1028.54(2)	20.3(8)	20.2(10)	20.6(8)	

^a From Ref. 14. The intensities are normalized to present value for the 984.45-keV γ ray.

^b From Ref. 14 unless otherwise noted.

^c Photons per hundred decays of ^{238}Np , normalized as described in the text. The uncertainties do not include a 3% uncertainty in the normalization factor.

^d The present values are adopted unless otherwise noted.

^e From the measured photon intensity and measured or theoretical internal conversion coefficients. (The intensity of the 44.08-keV transition is derived from the intensity of the M line and the theoretical conversion coefficients.)

^f Adopted value 0.099(5) from I_M and the theoretical conversion coefficients.

^g Weighted average of the present values measured in ^{238}Np and ^{242}Cm decay, and the value of Winter *et al.* (Ref. 14).

^h From the present measurement (^{238}Np decay).

ⁱ From the present measurement (^{242}Cm decay).

^j Weighted average of the present measurement (^{238}Np decay) and the value of Winter *et al.* (Ref. 14).

^k Doublet: $I_\gamma=0.065$ and $I_\gamma\approx 0.009$ for the $0, 3^- \rightarrow 0, 2^+$ and $0, 5^- \rightarrow 0, 4^+$ transitions, respectively. See Sec. III A.

^l Weighted average of the present values measured in ^{238}Np and ^{242}Cm decay.

^m From the intensity of the 837.18-keV γ ray and the branching ratio $\gamma_{939}/\gamma_{837}$ measured in ^{242}Cm decay

ⁿ Not placed in the decay scheme.

compares them to the previous work.¹⁴ In general, there is good agreement. The energies of most γ rays above 900 keV measured by Winter *et al.*¹⁴ are more precise, and have been adopted. Below 900 keV, the two sets of energies are of comparable precision; I have adopted averages that take into account also the γ -ray energies measured in the decay of ²⁴²Cm. Column 3 lists the adopted energies.

The γ -ray intensities measured in the present work (column 4 of Table I) are in agreement with those measured previously (column 5). I have adopted the present results for use in the following discussion. The intensities in column 4 are in units of photons per 100 decays, normalized by equating the sum of the total ($\gamma + e^-$) intensity of the ground state transitions to 100%. This normalization yields an absolute intensity of $(27.8 \pm 0.8)\%$ for the 984.45-keV γ ray, in poor agreement with a directly measured value,¹⁵ $(23.8 \pm 0.6)\%$. [The present determination of the absolute intensity is sensitive to the assumed theoretical values for $\alpha_K(1028.54)$ and the M/total ratio for the 44.08-keV transition, as well as the measured ratio of conversion-line intensities $M(44.08)/K(1028.54)$. Although the direct measurement might be preferred, the value was never published.] Note that the uncertainties in column 4 do not include the uncertainty in the absolute normalization, nor do the values in column 5, which have been normalized to 27.8 units for the 984.45-keV γ ray to facilitate comparison.

Transition intensities listed in the last column of Table I are based on the photon intensities, on conversion-electron intensities measured in the present experiment, and on theoretical internal conversion coefficients.¹⁶ A portion of the conversion-electron singles spectrum is shown in Fig. 3. The electron spectrum was also measured, with poorer statistics, in coincidence with K x rays (+ 101.90-keV γ rays). The coincidence measurement suppresses both the high-energy β^- continuum and the L, M, N, \dots , lines, making it possible to observe some weak lines and to identify K lines masked by L or M lines. Table II gives the resulting conversion coefficients, normalized to the theoretical K -conversion coefficient for the 1028.54-keV $E2$ transition. Because of the higher precision of the present conversion coefficients, I have not listed the previous data,¹⁴ which are in agreement. The present results provide data on 7 weak transitions whose conversion coefficients have not been measured previously in the decay of ²³⁸Np. (Conversion coefficients of several of the transitions were measured in the decay of ²³⁸Am.¹⁷) These include 4 interband transitions between odd-parity bands, for which the

$E2/M1$ mixing is determined. Precise conversion coefficients for the strong transitions from the gamma-vibrational band establish low limits on possible $M1$ admixtures. The weak 941.5 K line, observed as a shoulder on the 938.95 K line (Fig. 3), is assigned as the $0, 0^{+'} \rightarrow 0, 0^+$ pure $E0$ transition. Although its energy corresponds to that of the 941.38-keV γ ray, the K -conversion intensity of the latter transition, whose multipolarity is $E1$ according to the decay scheme, is expected to be only 2% of the intensity of the observed line. Multipolarities based on the conversion data are given in the last column of Table II.

Nine transitions are observed for the first time in the present study. All except the 220.87-keV transition are placed readily in the level scheme of ²³⁸Pu. Although this weak transition could be due to impurities in the γ -ray and electron spectra, the observation of K and L lines at the expected energies (± 0.5 keV) is evidence that the transition is converted in Pu. Its conversion coefficients are consistent with a pure $M2$ multipolarity.

Figure 4 shows the decay scheme for ²³⁸Np. Since this scheme does not differ significantly from that proposed previously,^{14,17} only the new features are discussed here. New transitions are placed as follows. The 157.42-keV $0, 6^+ \rightarrow 0, 4^+$ transition is well established from the decay of ²⁴²Cm. In ²³⁸Np decay, the $0, 6^+$ state is fed by the 459.8-keV transition from the $0, 5^-$ state at 763.27 keV, which has been observed for the first time in the present study. This state also decays by a 617.3-keV $0, 5^- \rightarrow 0, 4^+$ transition that is masked by the stronger $0, 3^- \rightarrow 0, 2^+$ transition; its γ -ray intensity is estimated to be 3.0 times that of the $0, 5^- \rightarrow 0, 6^+$ photon from an analysis of the band structure (see Sec. IVA). The $0, 5^-$ state is fed by the 319.29-keV transition from the 1082.59-keV $4, 4^-$ state; a zero intensity balance (within

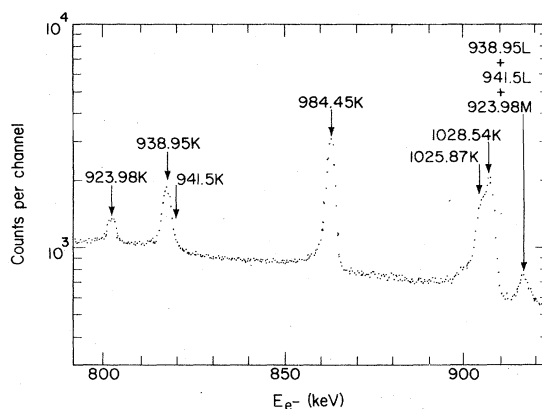


FIG. 3. Partial conversion-electron spectrum of ²³⁸Np.

TABLE II. Internal conversion coefficients in the decay of ^{238}Np .

E_γ (keV)	Shell	Experimental	Internal Conversion Coefficient ^a					Assigned multiplicity ^b
			E_1	E_2	E_3	M_1	M_2	
44.08	M^c	175(20)	0.216	162	10 800	12.2	741	E_2
101.90	L	11.2(6)	0.0959	10.7	258	4.31	62.6	E_2
	$(L_1+L_2)/L_3$	1.61(5)	3.10	1.63	1.94	226	4.22	
119.9	L^d	2.8(6)	0.0626	5.00	105	2.68	31.4	$M_1, <13\% E_2$
	M	0.69(6)	0.0153	1.40	32.3	0.652	8.63	
	N	0.23(3)						
220.87	$K^{e,f}$	6.7(15)	0.0646	0.132	0.296	2.36	7.60	$M_2?$
	L^g	4.0(10)	0.0136	0.344	4.21	0.473	2.81	
319.29	K^e	0.49(20)	0.0289	0.0702	0.180	0.851	2.34	$M_1 + 46(26)\% E_2$
323.98	K	0.17(5)	0.0280	0.0684	0.175	0.817	2.24	$M_1 + 86(7)\% E_2^h$
357.62	K	0.13(2)	0.0228	0.0572	0.148	0.623	1.65	$M_1 + 87.0(35)\% E_2^i$
882.63	K	0.0115(8)	0.004 10	0.0116	0.0263	0.0554	0.120	E_2
918.69	K^e	0.0036(8)	0.003 83	0.0108	0.0244	0.0499	0.108	E_1
923.99	K	0.0099(4)	0.003 79	0.0107	0.0241	0.0491	0.106	E_2^j
938.95	K	3.5(4)	0.003 68	0.0104	0.0234	0.0471	0.101	$E_0 + E_2, M_1$
	K/L	5.2(2)	5.75	3.69	2.36	5.14	4.38	
941.5		$I_K = 0.0094(7)$						E_0
962.77	K^e	0.0021(10)	0.003 53	0.009 96	0.0223	0.0441	0.0949	E_1
984.45	K	0.0096(3)	0.003 39	0.009 58	0.0213	0.0415	0.0894	$E_2, <3\% M_1$
	K/L	4.4(2)	5.77	3.81	2.49	5.15	4.42	
	$(L_1+L_2)/L_3$	19(2)	20.1	18.6	20.7	286	83.6	
	L/M	3.4(2)						
1025.87	K	0.0091(4)	0.003 16	0.008 92	0.0197	0.0373	0.0801	$E_2, <3\% M_1$
	K/L	4.3(3)	5.78	3.92	2.61	5.15	4.45	
1028.54	K	(0.008 88)		0.008 88				E_2
	K/L	4.2(2)	5.79	3.92	2.61	5.15	4.45	

^a Experimental values from the present measurements, normalized to the theoretical $\alpha_K(E_2)$ value for the 1028.54-keV transition. Theoretical values are interpolated from the tables of Hager and Seltzer (Ref. 16).

^b From the measured conversion coefficients.

^c The L lines of the 44.11-keV transition were also measured, but the line-shape analysis is less certain.

^d Corrected for an 80% contribution from the 101.90 M lines.

^e From the e^- - KX coincidence spectrum.

^f Corrected for a 25% contribution from the 101.90 N lines.

^g Corrected for a 22% contribution from the 319.29 K line.

^h Ahmad *et al.* (Ref. 17) assign a pure M_1 multiplicity from approximate L_{I+II} and M conversion coefficients measured in the decay of ^{238}Am , in disagreement with the present result.

ⁱ Ahmad *et al.* (Ref. 17) calculate the E_2 content as 83% from the measured K^- , L_{I+II^-} , L_{III^-} , and M -conversion coefficients, in agreement with the present results.

^j May contain a contribution from a second (E_1) γ ray of energy ≈ 924 keV. See text.

uncertainty) is calculated for the $0, 5^-$ state, consistent with the expected absence of direct β^- feeding. New transitions of energy 321.75 and 378.05 keV deexcite the well-established $0, 2^{+7}$ state. Transitions of energy 897.33 and 941.5 keV (E_0) deexcite the $0, 0^{+7}$ member of this band; although not observed in previous studies of ^{238}Np , they are well established from the decay of ^{242}Cm . A 336.38-keV γ ray, which also deexcites this state, is too weak to have been observed in the decay of ^{238}Np ; its intensity and that of the 983.0-keV $0, 2^{+7} \rightarrow 0, 0^+$ γ ray, which is masked by the much stronger 984.45-keV γ ray, are calculated from the branching ratios measured in the decay of ^{242}Cm . A tentative level at 968.2 keV was pro-

posed in previous studies.^{18,14} The present measurements neither support nor refute its existence; it is shown in Fig. 4 for completeness.

B. ^{242}Cm decay

Gamma-ray energies and intensities for ^{242}Cm are shown in Table III. Because of possible self-absorption and interference from ^{243}Cm decay, the spectrum below 300 keV was not studied exhaustively, and the intensities of the $0, 6^+ \rightarrow 0, 4^+$ and $0, 4^+ \rightarrow 0, 2^+$ transitions are not quoted. The absolute intensity of the 561.11-keV γ ray is estimated to be $(1.5 \pm 0.4) \times 10^{-40\%}$ from the relative intensities and a previous $\alpha\gamma$ coincidence determination of the sum of the absolute inten-

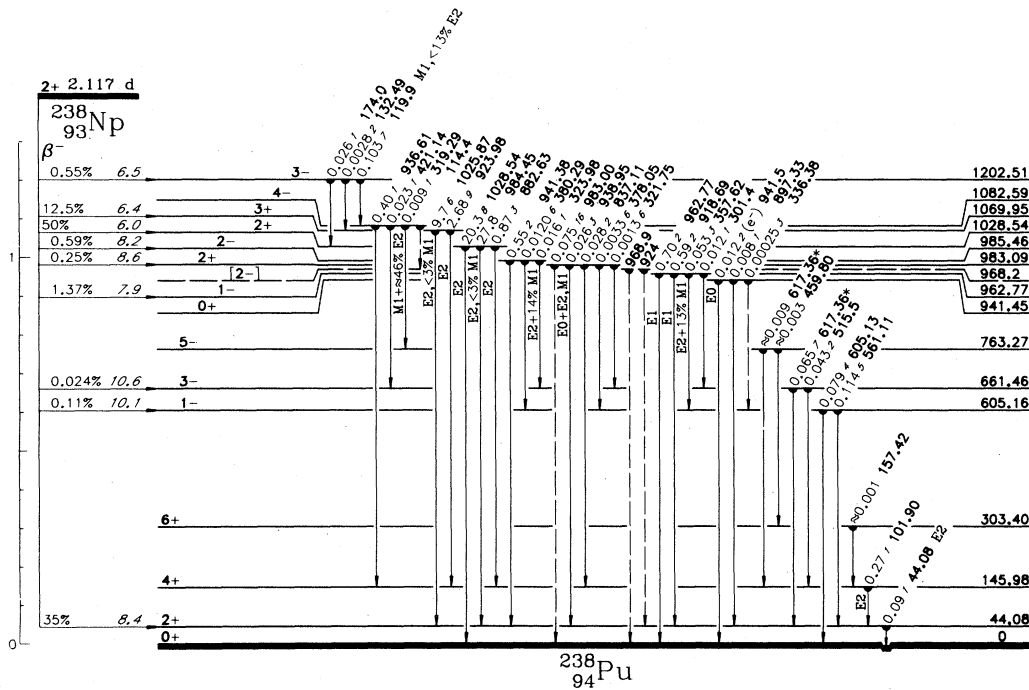


FIG. 4. Decay scheme of ^{238}Np . Energies and intensities are adopted values from the present work and Ref. 14. Energies are shown in bold type, absolute photon and β^- intensities in lighter type. Italic numbers to the right of the β^- intensities are $\log ft$ values.

sities of the 515.25-, 561.02-, 605.04-, and 617.22-keV γ rays.¹⁹

Gamma rays have been assigned to the decay of ^{242}Cm on the basis of rotational bands in ^{238}Pu known from the decay of ^{238}Np and ^{238}Am . Weak γ rays in the spectrum can be due to ^{242}Cm decay, or to spontaneous fission (that is, to the deexcitation of fission fragments, or to the β^- decay of fission products). The maximum possible intensity of a fission γ ray is $0.1 \times \text{SF}/\alpha = 7 \times 10^{-9}$ per α decay, equivalent to 0.5 units on the relative intensity scale of Table III. Several γ rays in the observed spectrum can be identified with known fission products, and many others are assigned to the fission mode by comparison with the spectrum of ^{240}Pu , which has a similar SF/α ratio but weaker γ rays associated with the α -decay mode.^{14,20} On the basis of this comparison, it is very unlikely that even the weakest γ rays in Table III are associated with the spontaneous fission mode.

The decay scheme is shown in Fig. 5. Energies of the γ -ray transitions shown on the scheme are adopted values, as described in Sec. III A. New levels of ^{238}Pu are established at 1018.6 and 1175.8 keV. Alpha-decay hindrance factors shown in Fig. 5 are calculated from the one-body, spin-independent model of Preston.²¹

TABLE III. Gamma rays of ^{242}Cm .

E_γ (keV)	I_γ relative
101.93(4)	a
157.42(5)	a
336.38(15)	0.45(15)
358.0(5)(?) ^c	0.39(13)
459.80(2)	0.038(16)
515.25(19)	2.97(20)
561.02(10)	100
605.04(10)	69.8(20)
617.22(12)	5.36(20) ^b
837.01(15)	0.124(20)
897.33(10)	14.5(10)
918.7(2)	0.36(3)
938.91(10)	0.117(20)
962.8(2)	0.35(3)
974.5(3)(?)	≤ 0.13
979.80(20)	0.173(30)
983.00(30)	0.33(8)
984.5(1)	1.31(20)
1028.5(2)	1.05(10)
1081.70(30)	0.033(10)
1118.26(30)	0.11(5)
1184.64(30)	0.33(4)
1220.19(30)	0.187(30)

^a Not measured.

^b Complex. According to the analysis in Sec. IV B, the intensity can be decomposed as follows:

$$0, 3^- \rightarrow 0, 2^+ 5.25,$$

$$0, 5^- \rightarrow 0, 4^+ 0.11.$$

^c Not placed in the decay scheme.

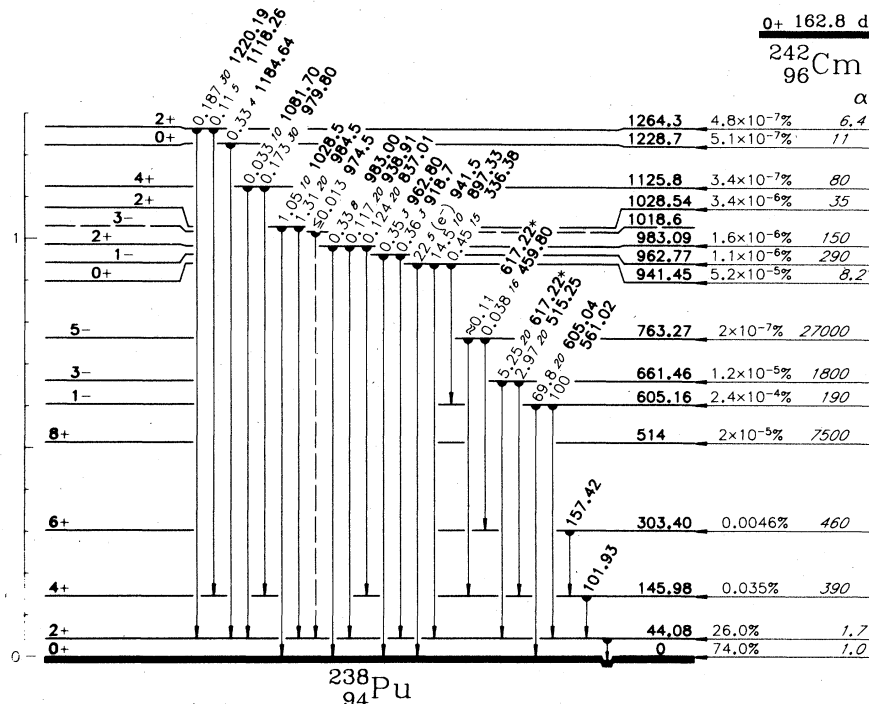


FIG. 5. Decay scheme of ^{242}Cm . Energies are shown in bold type, relative photon and absolute α intensities in light-type. Italic numbers to the right of the α intensities are hindrance factors, calculated with the one-body equations of Preston (Ref. 21).

IV. DISCUSSION

A. E1 transition rates in ^{238}Pu ; the rotation-admixing model

Rotational transition rates are given by the expression²²

$$B(E2) = \frac{5}{16\pi} e^2 Q_0^2 \langle I_i K_i 20 | I_f K_f \rangle^2, \quad (1)$$

where Q_0 is the intrinsic quadrupole moment, and $\langle I_i K_i 1 K_f - K_i | I_f K_f \rangle$ is the vector-addition coefficient. With an assumption about the variation of Q_0 from one band to another and from nucleus to nucleus, rotational transitions can serve as standards with "known" transition rates, against which one can measure the half-lives of the states they deexcite and the rates of competing transitions. In the calculations that follow, the value of Q_0 for the $0, 2^+ \rightarrow 0, 0^+$ ground-state transition of an even-even nucleus is used for all rotational transitions in the same nucleus. By use of this assumption, Bohr and Mottelson estimated the rate of the $0, 3^- \rightarrow 0, 2^+$ E1 transition, in competition with the $0, 3^- \rightarrow 0, 1^-$ rotational transition in ^{228}Th .²³ (The existence of the rotational transition upon which this calculation was based is not confirmed in more recent experiments.⁸) Recently,

Kurcewicz *et al.*²⁴ have applied the same technique in ^{224}Ra . In ^{238}Pu , rotational transitions have not been observed within the odd-parity bands. However, interband E2 transitions between the $K^\pi = 1^-$ and $K^\pi = 0^-$ bands also can serve as decay-rate standards, as is shown in the following discussion. These transitions occur by virtue of Coriolis mixing between states of the two bands, whose wave functions can be represented by

$$\phi_{\text{lower}}^I = \phi_{K=0}^I + a f(I) \phi_{K=1}^I, \quad (2)$$

$$\phi_{\text{upper}}^I = \phi_{K=1}^I - a f(I) \phi_{K=0}^I,$$

where I is the spin of the state,

$$f(I) = [I(I+1)]^{1/2}$$

and a is a variable (spin-independent) parameter representing the strength of the Coriolis coupling. [Since $|a| \ll 1$, I have omitted the coefficient $(1-a^2)^{1/2}$ of the larger terms in the wave functions.] The interband E2 transition probability is given by

$$B(E2) = \frac{5}{16\pi} e^2 Q_0^2 a^2 [f(I_f) \langle I_i 120 | I_f 1 \rangle - f(I_i) \langle I_i 020 | I_f 0 \rangle]^2, \quad (3)$$

where I_i and I_f are the spins of the initial and final states, respectively.

The mixing parameter a can be estimated from the $E1$ branching ratios as follows. The reduced branching from any member of the lower ($K=0$) band to a member of the ground-state band is given by

$$W(E1; I_i \rightarrow I_f) \propto [\langle I_i 010 | I_f 0 \rangle + z_0 f(I_i) \langle I_i 11 - 1 | I_f 0 \rangle]^2, \quad (4)$$

where

$$z_0 = a \frac{\langle 1^- \| E1 \| 0^+ \rangle}{\langle 0^- \| E1 \| 0^+ \rangle}$$

and $\langle K^- \| E1 \| 0^+ \rangle$ is the reduced (spin-independent) $E1$ transition rate. By use of this relationship, z_0 can be determined from the relative $E1$ branching from any member of the $K^\pi = 0^-$ band. Similarly, the reduced branching from any odd-spin member of the $K^\pi = 1^-$ band is given by

$$W(E1; I_i \rightarrow I_f) \propto [\langle I_i 11 - 1 | I_f 0 \rangle + z_1 f(I_i) \langle I_i 010 | I_f 0 \rangle]^2, \quad (5)$$

where

$$z_1 = -a \frac{\langle 0^- \| E1 \| 0^+ \rangle}{\langle 1^- \| E1 \| 0^+ \rangle}$$

from which it follows that

$$a = (-z_0 z_1)^{1/2} \quad (6)$$

and

$$\left| \frac{\langle 0^- \| E1 \| 0^+ \rangle}{\langle 1^- \| E1 \| 0^+ \rangle} \right| = (-z_1/z_0)^{1/2}. \quad (7)$$

In ^{238}Pu , the experimental $E1$ branching ratios from the $0, 1^-$ and $0, 3^-$ states yield a consistent value of $z_0 = -0.029 \pm 0.005$. [It should be noted that the $0, 3^- \rightarrow 0, 2^+$ γ ray (617.36 keV) masks the weaker $0, 5^- \rightarrow 0, 4^+$ γ ray of the same energy. The intensity of the latter γ ray is estimated from $I_\gamma(0, 5^- \rightarrow 0, 6^+)$ and Eq. (4), iterating on z_0 to obtain self-consistency. It is also possible to obtain purely experimental $E1$ branchings from the $0, 3^-$ and $0, 5^-$ states, by use of the γ -ray intensities measured in the decay of both ^{238}Np and ^{242}Cm , since the two parents populate the states in different proportions. Due to experimental uncertainties, this method yields only an upper limit for the intensity of the $0, 5^- \rightarrow 0, 4^+$ transition, which is consistent with the value adopted.] The $E1$ branching ratio from the $1, 1^-$ state yields $z_1 = 0.0819 \pm 0.0039$. From Eqs. (6) and (7),

$$|a| = 0.0485 \pm 0.0043$$

and

$$\left| \frac{\langle 0^- \| E1 \| 0^+ \rangle}{\langle 1^- \| E1 \| 0^+ \rangle} \right| = 1.69 \pm 0.15.$$

From Eqs. (1) and (3) (using a half-life⁸ 1.73×10^{-10} s for the $0, 2^+$ state of ^{238}Pu), the half-life of the 962.77-keV state is estimated to be $(6.2 \pm 1.2) \times 10^{-12}$ s; the partial half-life of the 962.77-keV $E1$ transition is 1.2×10^{-11} s, corresponding to a hindrance factor²⁵ $F_w = 6.0 \times 10^4$. Correction for the $\Delta K = 0$ component of the transition [Eq. (5)] yields

$$F_w^{\Delta K=1} = 4.7 \times 10^4.$$

Similar analysis of the $E1/E2$ competition in the decay of the 985.46-keV $1, 2^-$ state yields for the 941.38-keV transition

$$F_w = F_w^{\Delta K=1} = 3.9 \times 10^4.$$

An average value, $F_w^{\Delta K=1} = 4.3 \times 10^4$, is adopted for the band; from Eq. (7), one obtains $F_w^{\Delta K=0} = 1.5 \times 10^4$. Predicted half-lives of the states are summarized in Table IV.

B. $E1$ transition rates from octupole states in other heavy nuclei

The rotation-admixing model developed above can be used to estimate $E1$ transition rates in other nuclei for which sufficient data on relative branching are available. Results are presented in Table V. The following are comments on specific nuclei:

²²⁴Ra. The data are from Ref. 24. $F_w^{\Delta K=0}$ is derived from a direct comparison of the intensities of $E1$ transitions with the intensities of competing rotational transitions. The value given is the geometric mean of the values estimated for the $0, 3^- \rightarrow 0, 2^+$ and $0, 5^- \rightarrow 0, 4^+$ transitions, 0.6×10^4 and 2.4×10^4 , respectively. These values have been corrected for the $\Delta K = 1$ component of the transitions by use of the mixing parameter z_0 derived from the $E1$ branching from the $0, 1^-$ state. The estimates are not subject to possible

TABLE IV. Predicted half-lives of octupole states in ^{238}Pu .^a

Level		
Energy (keV)	K, I^π	$t_{1/2}$ (ps)
605.16	$0, 1^-$	4.7 ± 0.5
661.46	$0, 3^-$	3.7 ± 0.4
962.77	$1, 1^-$	6.2 ± 1.2^b
985.46	$1, 2^-$	5.3 ± 1.1^b

^a Based on the rotation-admixing model described in the text and the present experimental results.

^b Calculated directly from the decay of this state. The average value of F_w for the decay of the $1, 1^-$ and $1, 2^-$ states is equivalent to $t_{1/2}(962.77) = 5.7$ ps, $t_{1/2}(985.46) = 5.9$ ps.

TABLE V. Estimated E1 transition probabilities for octupole states ($K=0$ or 1) in nuclei with $Z \geq 88$.^a

Nucleus	z_0	z_1	$\frac{ a }{\langle 1^- H' 0^- \rangle}$, (keV)	$\left \frac{\langle 0^- E1 0^+ \rangle}{\langle 1^- E1 0^+ \rangle} \right $	$F_W^{\Delta K=0}$	$F_W^{\Delta K=1}$
²²⁴ Ra	+0.044(9)				1.2×10^4	
²²⁸ Th	+0.012(5)	-0.12	0.038 (23.6)	3.2	2×10^3	2×10^4
²³⁰ Th	+0.032	-0.079	0.050 (22)	1.57	4×10^3	9×10^3
²³⁶ U	+0.177(3)	-0.012	0.047 (13)	0.26	$\leq 4.5 \times 10^7$ (2.2×10^7) ^b	$\leq 3.1 \times 10^6$
²³⁸ U	-0.005(2)	+0.18(8)	0.030(9)	6(2)	9×10^4	3.2×10^6
²³⁸ Pu	-0.029(5)	+0.0819(39)	0.0485(43) (17(2))	1.69(5)	1.5×10^4	4.3×10^4

^a See Sec. IV B for a discussion of the data for each nucleus. Numbers in parentheses are uncertainties in the last place(s).

^b From the directly measured half-life of the $0, 1^-$ state.

violations of the model (see below), but no information is obtained about the $\Delta K=1$ transition rates. With the assumptions that the $K^\pi=1^-$ band lies at about 1 MeV and that the strength of the mixing between the $K^\pi=1^-$ and 0^- bands is about $\frac{1}{2}$ of the theoretical estimate [Eq. (10)] one can estimate that $F_W^{\Delta K=1} \simeq F_W^{\Delta K=0}$. It should be noted that the half-life estimates obtained here (0.27 ns for the $0, 3^-$ level, 0.11 ns for the $0, 5^-$ level) disagree with the published values calculated (apparently) by the same method.²⁴

²²⁸Th. z_0 is a weighted average of values for the $0, 1^-$, $0, 3^-$, and $0, 5^-$ states, derived from several measurements reported in Ref. 8. Although the $K^\pi=1^-$ band has been identified tentatively, some of the transitions by which it decays have not been observed. In order to estimate z_1 and thus the ratio of $\Delta K=0$ to $\Delta K=1$ E1 matrix elements, it was assumed that the strength of the mixing between the $K^\pi=1^-$ and 0^- bands is $\frac{1}{2}$ that predicted by Eq. (10). The E1 strength is calculated from the relative intensities of the $1, 1^- \rightarrow 0, 2^+$ and $1, 1^- \rightarrow 0, 3^-$ transitions.

²³⁰Th. The required data are known, but without uncertainty limits. The information in Table V is derived from several measurements of relative γ -ray intensities and E2/M1 mixing reported in Ref. 8. A consistent value of z_0 is derived from the E1 branching from the $0, 1^-$ and $0, 3^-$ states, of z_1 from the $1, 1^-$ and $1, 3^-$ states. The estimate for $F_W^{\Delta K=0}$ is the geometric mean of the values 1.7×10^4 , 0.9×10^4 , and 6.4×10^4 for the $1, 1^-$, $1, 2^-$, and $1, 3^-$ states, respectively.

²³⁶U. The data, derived from the decay of ²³⁶Pa and ²³⁶Np and the reaction ²³⁵U($d, p\gamma$), are summarized in Refs. 8 and 1. The value of z_1 , -0.012 ,

is derived from the branching from the $1, 1^-$ state; the branching from the $1, 3^-$ state yields $z_1 = +0.061$, which is inconsistent with this value and with the rotation-admixing model, which requires that z_1 and z_0 have opposite signs [see Eqs. (6) and (7)]. The E2 content of the rotation-admixed transitions is unknown; the calculations are based on the assumption that they are pure E2 transitions, and thus provide upper limits for the hindrance factors F_W . $F_W^{\Delta K=1}$ is derived from the E1/E2 competition in the decay of the $1, 1^-$ state; the value (Table V) is consistent with the approximate value $\leq 1.5 \times 10^6$ derived from the decay of the $1, 2^-$ state. There is close agreement between the estimate for $F_W^{\Delta K=0}$ and the experimental value derived from the directly measured half-life of the $0, 1^-$ state. On the other hand, the inconsistency of the z_1 values noted above is a serious violation of the model. This problem is considered further in Sec. IV C.

²³⁸U. The data are derived mainly from unpublished Coulomb-excitation results.^{26,27} The value of z_0 , -0.005 ± 0.002 , is calculated from the precisely measured E1 branching from the $0, 3^-$ state; the value derived from the $0, 1^-$ state branching ($+0.03 \pm 0.01$) has the opposite sign, although the two values differ by only about three standard deviations combined error. The value of z_1 is a simple average (with expanded uncertainty limit) of the values derived from the branching from the $1, 1^-$ and $1, 3^-$ states, $+0.23 \pm 0.02$ and $+0.13 \pm 0.01$, respectively. $F_W^{\Delta K=1}$ is an average of the values 3.0×10^6 for the $1, 1^-$ state and 3.4×10^6 for the $1, 2^-$ state. It is inconsistent with the value 1.2×10^5 deduced from the E1/(inter-band-E2) branching from the $1, 3^-$ state.

According to Ref. 26, rotational transitions compete with interband transitions in the deexcitation of the $0, 3^-$ and $1, 3^-$ states. (The rotational transitions have not been observed directly. Their intensities are inferred from the strength of the indirect Coulomb excitation of the $0, 1^-$ and $1, 1^-$ states.) The $E1$ /(intraband- $E2$) branching ratios from the two 3^- states yield $F_{\omega}^{\Delta K=1} = 1.0 \times 10^5$, $F_{\omega}^{\Delta K=0} = 5 \times 10^4$. These values are in agreement with the values deduced from the rotation-admixing model. Both methods support the conclusion that the $\Delta K=1$ transitions from the $1, 3^-$ state are less hindered than those from lower-spin members of the same band.

C. Validity of the rotation-admixing model

The model described above involves assumptions that the interband $E2$ transitions are due to the mixing between the bands containing the initial and final states, and that the strength of this mixing can be estimated from the $E1$ branching ratios. The first assumption is supported by the following considerations:

(1) The interband $E2$ transitions have estimated strengths of approximately one single particle unit. It is unlikely that any transition between intrinsic (Nilsson) states would be this fast. In fact, calculations of $E2$ strengths in deformed nuclei are commonly made under the assumption that the $E2$ transitions result from rotational admixtures.

(2) Any admixtures other than those between members of the initial and final bands would result in $E2$ strengths proportional to $a^{(p+4)}$, whereas the postulated transitions have strengths proportional to a^2 . Because the mixing parameter a is approximately 0.05, rotational transitions due to other admixtures would be at least 400 times slower.

(3) The observed branching ratios of the interband $E2$ transitions are consistent (but not exclusively so) with Eq. (3). For example, the calculated value for $W_{\gamma}(E2; 1, 1^- \rightarrow 0, 3^-)/W_{\gamma}(E2; 1, 1^- \rightarrow 0, 1^-)$ is $\frac{2}{3}$; experimental values are 0.62 for ^{230}Th and 0.61 ± 0.07 for ^{238}Pu .

The derivation of the mixing parameter a from experimental $E1$ branching ratios is subject to a number of problems noted in the discussion of individual cases (Sec. IV B): The observed values of z_0 and z_1 do not all have opposite signs, as required by Eqs. (6) and (7), and inconsistent values of z_1 are obtained in some cases from the analysis of the branching from different members of the same band. However, there are other methods for estimating the strength of the inter-

band mixing. For the purpose of comparison, it is convenient to quote the Coriolis matrix element $|\langle K^{\pi}=1^- \| H' \| K^{\pi}=0^- \rangle| = |a\Delta E|$, where ΔE is the energy spacing between the two bands (taken to be the spacing between the bandheads). Based on the $E1$ branching ratios [Eq. (6)], the magnitude of this quantity is given by

$$|\langle 1^- \| H' \| 0^- \rangle| = (-z_0 z_1)^{1/2} \Delta E. \quad (8)$$

From the compression of the rotational spacing of the $K^{\pi}=0^-$ band,

$$|\langle 1^- \| H' \| 0^- \rangle| = \{[A(gsb) - A(0^-)]\Delta E\}^{1/2}, \quad (9)$$

where

$$A = \frac{\hbar^2}{2\mathcal{I}_0}$$

is the rotational constant for the band. From a theoretical (Coriolis) estimate,²²

$$\langle 1^- \| H' \| 0^- \rangle = \sqrt{24}A(gsb). \quad (10)$$

The estimate represented by Eq. (8) may be too high, too low, or meaningless (i.e., imaginary) because of mixing with other bands. (The $K^{\pi}=1^-$ band is more likely to contain other admixtures, since it occurs near the pairing gap, and thus probably lies close to other 0^- bands.) Equation (9) represents an upper limit to the mixing, provided the 0^- band does not have a larger deformation than the ground-state band. [This condition probably is not met in ^{224}Ra and, perhaps, in ^{228}Th , in which small rotational constants of the $K^{\pi}=0^-$ band relative to those of the corresponding ground-state bands and deviations from the systematic relationship between estimates given by Eqs. (9) and (10) suggest that the octupole band is more deformed.] Equation (10) is a rough estimate of the maximum Coriolis effect, and may be taken to be an approximate upper limit.

Table VI compares the matrix elements calculated by the three methods. Equations (8)–(10) yield comparable results, and the matrix elements are approximately constant from one nucleus to the next. The agreement adds some confidence

TABLE VI. Estimates of the mixing between the $K=0$ and $K=1$ octupole bands.

Nucleus	$ \langle 1^- \ H' \ 0^- \rangle $ (keV) estimated by:		
	Eq. (8)	Eq. (9)	Eq. (10)
^{224}Ra		72 ^a	69
^{228}Th		43	47
^{230}Th	22	33	43
^{236}U	13	23	37
^{238}U	8	25	37
^{238}Pu	17	25	36

^a If $E(1, 1^-) = 1000$ keV.

to the results presented in Table V. A value of $\frac{1}{2}$ the Coriolis estimate [Eq. (10)] has been used in the above discussion where sufficient data are lacking to use Eq. (8). The same estimate would probably be better than the one used for ^{238}U in Table V; i.e., the matrix element and the mixing parameter a should be about twice as large, and $F_W^{\Delta K=1}$ about $\frac{1}{4}$ as large as the values tabulated.

Except as otherwise noted, the above discussion assumes that the octupole bands are well behaved, i.e., that the reduced matrix elements are spin independent. This is not necessary assumption of the model, and the analysis indicates that the $\Delta K=1$ E1 matrix elements in ^{238}U are larger for the decay of the $1, 3^-$ state than for the decay of the $1, 1^-$ and $1, 2^-$ states. Similarly, the decay of the $0, 3^-$ and $0, 5^-$ states of ^{224}Ra are characterized by different values for the reduced $\Delta K=0$ matrix elements. The latter conclusion does not depend on assumptions of the rotation-admixing model, since the estimates for ^{224}Ra are based on a direct comparison with rotational transitions.

V. CONCLUSION

Hindrance factors for E1 transitions from octupole states in the Ra–Pu region vary from 2×10^5

to 2×10^7 . Especially dramatic is the variation of over two orders of magnitude in the $\Delta K=0$ transition rate between ^{236}U and ^{238}U , and over three orders of magnitude between the isotones ^{236}U and ^{238}Pu . The variation in $\Delta K=1$ transition rates is only slightly smaller, and the ratio of $\Delta K=0$ to $\Delta K=1$ transition rates varies sharply in this region. It is possible to interpret the results as a relatively smooth trend interrupted by an anomaly at $^{236-238}\text{U}$. By contrast, the E1 transitions in gadolinium and dysprosium isotopes behave quite regularly, with $F_W^{\Delta K=0}$ on the order of 400, $F_W^{\Delta K=1}$ on the order of 3×10^5 .²⁸

ACKNOWLEDGMENTS

I should like to thank Jim Harris for assistance with source preparation, and Mike Kelley, Dirk Benson, and Dick Meyer for assistance with the measurements. This work was supported by the Office of Energy Research, the Office of Basic Energy Sciences, and the Division of Nuclear Sciences of the U.S. Department of Energy under Contract No. W-7405-ENG-48.

- ¹H. F. Brinckmann, D. D. Clark, N. J. S. Hansen, and J. Pedersen, *Phys. Lett.* **43B**, 386 (1973).
²J. S. Boyno, J. R. Huizenga, Th. W. Elze, and C. E. Bemis, Jr., *Nucl. Phys.* **A209**, 125 (1973).
³F. K. McGowan, C. E. Bemis, Jr., W. T. Milner, J. L. C. Ford, Jr., R. L. Robinson, and P. H. Stelson, *Phys. Rev. C* **10**, 1146 (1974).
⁴C. M. Lederer, J. M. Jaklevic, and S. G. Prussin, *Nucl. Phys.* **A135**, 36 (1969).
⁵W. L. Posthumus, K. E. G. Lobner, J. L. Maarleveld, H. P. Geerke, and J. Konijn, *Z. Phys. A* **281**, 277 (1977).
⁶F. Asaro, F. S. Stephens, J. M. Hollander, and I. Perlman, *Phys. Rev.* **117**, 492 (1960).
⁷I. Ahmad, R. K. Sjoblom, A. M. Friedman, and S. W. Yates, *Phys. Rev. C* **17**, 2163 (1978).
⁸*Table of Isotopes*, 7th ed., edited by C. M. Lederer and V. S. Shirley (Wiley, New York, 1978).
⁹W. Donner and W. Greiner, *Z. Phys.* **197**, 440 (1966).
¹⁰A. Faessler, T. Udagawa, and R. K. Sheline, *Nucl. Phys.* **85**, 670 (1966).
¹¹G. Monsonogo and R. Piepenbring, *Nucl. Phys.* **78**, 265 (1966).
¹²L. K. Peker and J. H. Hamilton, *J. Phys. G* (London) **5**, L165 (1979).
¹³L. J. Jardine and C. M. Lederer, *Nucl. Instrum. Methods* **120**, 515 (1974).
¹⁴W. J. B. Winter, A. H. Wapstra, P. F. A. Goudsmit, and J. Konijn, *Nucl. Phys.* **A197**, 417 (1972); *ibid.* **A161**, 521 (1971).
¹⁵R. P. Schuman, Idaho Nuclear Corp. Report IN-1126, 1967, p. 19 (unpublished).
¹⁶R. S. Hager and E. C. Seltzer, *Nucl. Data* **A4**, 1 (1968).
¹⁷I. Ahmad, R. K. Sjoblom, R. F. Barnes, F. Wagner, Jr., and P. R. Fields, *Nucl. Phys.* **A186**, 620 (1972).
¹⁸B. Bengtson, J. Jensen, M. Moszynski, and H. L. Nielsen, *Nucl. Phys.* **A159**, 249 (1970).
¹⁹C. M. Lederer, Ph.D. thesis, University of California Radiation Laboratory Report UCRL-11028, 1963 (unpublished).
²⁰C. M. Lederer, unpublished data reported in Ref. 8.
²¹M. A. Preston, *Phys. Rev.* **71**, 865 (1947).
²²A. Bohr and B. R. Mottelson, *Nuclear Structure* (Benjamin, Reading, Massachusetts, 1969), Vol. II.
²³A. Bohr and B. R. Mottelson, *Nucl. Phys.* **4**, 529 (1957).
²⁴W. Kurcewicz, N. Kaffrell, N. Trautmann, A. Plochocki, J. Zylicz, M. Matul, and K. Stryczniewicz, *Nucl. Phys.* **A289**, 1 (1977).
²⁵Hindrance factors are defined relative to a modified Weisskopf single-particle estimate:

$$\lambda_{\text{SP}} = 1.0 \times 10^{14} A^{2/3} E_\gamma^3 \frac{\langle I_i K_i | 1 K_f - K_i | I_f K_f \rangle^2}{\frac{1}{3}}$$
where E_γ is the γ -ray energy in MeV, the vector-addition coefficient is included to make the estimate spin-independent, and the factor $\frac{1}{3}$ [$= \langle 1 K_i 1 - K_i | 0 0 \rangle^2$] is included to normalize to the conventional Weisskopf estimate for ground-state transitions.
²⁶Y. A. Ellis, *Nucl. Data Sheets* **21**, 549 (1977).
²⁷F. K. McGowan, private communication.
²⁸F. K. McGowan and W. T. Milner, *Phys. Rev. C* (to be published).